Life Cycle Costing Based Design Optimization and Viability Analysis of the Adoption of the Hybrid Technology in Philippines Tricycles

Jose Bienvenido Manuel M. Biona[1*] and Alvin B. Culaba[1]

[1]**Mechanical Engineering Department, De La Salle University - Manila**

The acceptability of the hybrid electric vehicle (HEV) technology in Philippine tricycles will be defined by its economic viability. This study investigated the optimum HEV component and control variable combination that will provide the most incremental life cycle cost benefits relative to the current conventional tricycle power train. Simulations were implemented using an instantaneous vehicle model specifically developed for Philippine tricycles and based on local drive cycles. Its viability was evaluated vis-a-vis projected technology developments and component price reductions. Results indicated that the 60 cc ICE, 8.66 kW_{peak} and 0.47 kWh battery configuration will provide the best fuel economy and highest financial feasibility while the 70 cc and 80 cc systems may also be adopted should lower capital cost is desired. Viability is strongly dependent on future fuel oil prices and is not expected before 2020.

KEYWORDS

Hybrid Electric Vehicles, Life Cycle Costing, Tricycles, Vehicle Design Optimization, Vehicle Instantaneous Modeling

*Corresponding author
Email Address : bionaj@dlsu.edu.ph
Received: Aug 16, 2009
Revised: Feb 15, 2010
Accepted: Feb 27, 2010
Published: March 30,2010

INTRODUCTION

There are approximately 1.8 million tricycles in the Philippines serving as a major means of public transport in the country. In Quezon City alone, it accounts for about 4 million person-trips made daily with a variety of trip purposes ranging from home, business, school or work trips (Garcia et al. 2007). Driving these vehicles has become a major means of living among the marginalized sector both in urban and rural areas. These vehicles however are mostly powered by two stroke engines which are commonly known for their high hydrocarbon and particulate emissions. Most local government units have already banned the registration of new two stroke powered tricycles and have advocated a number of interventions including shifting to four strokes, adoption of the direct injection retrofitting technology and utilization of alternative fuels. To ensure greater environmental sustainability, more advanced and cleaner vehicle technologies should be explored for the long term considering the sheer number of these vehicles. These include hybrid and electric vehicle technologies.

Previous studies have mostly looked at optimizing HEV designs based on fuel consumption and in-use emission reduction (Barsali et al. 2004; Assanis et al. 1999; Johnson et al. 2000; Lin et al. 2003; Arsie et al. 2004; Montazeri-Gh and Poursamad 2006; Baumann et al. 2000; Shouten et al. 2002). This approach is not able to take into account differences in vehicle production and maintenance phase environmental impacts which could possibly be significant. Battery replacement impact is of particular interest considering the rare materials and toxic components involved. Considering however the limited purchasing capability of the tricycle sector, the

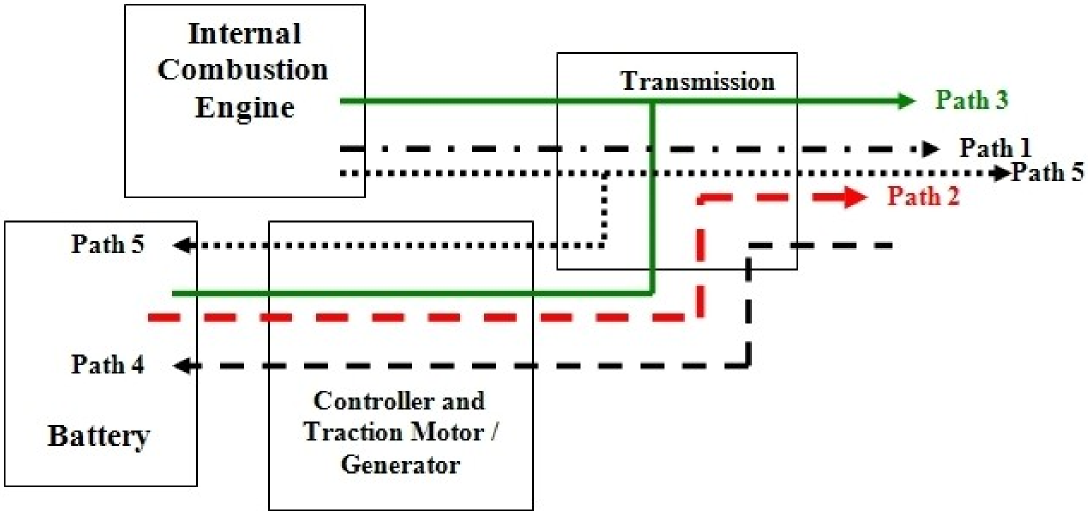

Figure 1. HEV power train diagram and energy path

acceptability of these technologies strongly hinges on their economic viability. It could be said though that the factors affecting the economics of such vehicles also define their life cycle assessment performance (Rebitzer et al. 2002; Senthil et al. 2003). Higher power train cost normally translates to higher material resource depletion, extraction and component production impacts (Wang 2007). Higher fuel savings are equated to lower fuel upstream environmental implications and in-use emissions. Smaller capacity and less frequent battery capacities bring down resource depletion and toxic material discharges. This study aimed to determine the optimum HEV component and control parameter combination that would provide the most incremental life cycle cost benefits relative to the 175 cc four stroke drive trains. It also seeks to determine when the technology will be viable for tricycles.

MATERIALS AND METHODS

System Configuration and Power Management Strategy

A parallel hybrid electric vehicle system shown in Figure 1 was adopted in the study. The internal combustion engine (ICE) and electric motor (EM) power are combined by a gear assembly upstream of the transmission.

The operation of the system is defined by the control variables listed in Table 1.

The baseline strategy uses the engine as the primary power source (see path 1 in Figure 1) and uses the motor as follows:

1. The motor supplies all driving torque (see path 2 in Figure 1) when the instantaneous torque fraction requirements are below :

Table 1. Control strategy state variables

Variable	Description
SOC_{max}	Highest desired battery State of Charge (SOC). Set at 0.8 in this study.
SOC_{min}	Lowest desired battery SOC. Determined as 0.8-ΔSOC in this study where ΔSOC is varied from 0.05 to 0.45.
$T_{o\text{-}normal}$	Torque fraction below which the motor will power the vehicle when the battery is between SOC_{max} and SOC_{min}. Torque fraction is the ratio of the instantaneous engine torque demand with the engine peak torque.
$T_{o\text{-}high}$	Torque fraction below which the motor will power the vehicle when the battery is above SOC_{max}.

- $T_{o\text{-}normal}$ when Battery SOC is between maximum (SOC_{max}) and minimum (SOC_{min}) state of charge.
- $T_{o\text{-}high}$ when Battery SOC is above SOC_{max}.

2. The motor assists the ICE if the required torque exceeds the maximum engine torque at the operating rpm (see path 3 in Figure 1).
3. The motor acts as a generator and charges the battery during:
   - Regenerative braking modes (see path 4 in Figure 1).
   - When battery falls below SOC_{min} , charging power will be supplied by the ICE operated at its most efficient torque point at the current engine speed. This will be implemented only if the torque required is less than the maximum efficiency torque point (see path 5 in Figure 1).

The average efficiency at the most efficient torque point for the different engine speeds was found to be around 92% relative to the highest efficiency point. With an average roundtrip EM drive train efficiency of 83% (see discussions below) for ICE charged power path, the EM drive train should thus be used if the ICE efficiency (relative to the highest efficiency point) is 77% or less except in the power assist mode (see path 2). Beyond this efficiency point, running the vehicle using the ICE becomes more efficient. This corresponds to a 30% torque fraction based on the engine mapping approach adopted. As such, $T_{o\text{-}high}$ was set to 30%. $T_{o\text{-}normal}$ on the other hand was set at 15%. Utilizing higher or lower $T_{o\text{-}normal}$ led to unacceptable $SOC_{s\text{-}e}$.

Problem Formulation

The study focused on determining the drive train component and control variable combinations that would provide the maximum incremental life cycle cost benefits (ICB) relative to four stroke powered systems. Currently, four stroke tricycles are mostly sized at 175 cc. Optimization variables accounted include internal combustion engine size (ICE_{cc}), traction motor peak power (TM_{pp}), battery storage capacity ($Bat_{storage}$) and state of charge operational range (ΔSOC). The SOC operational range represents the desired region where the battery state of charge is supposed to be maintained. It is the difference between SOC_{max} and SOC_{min} .

$$Max\ ICB = f(ICE_{cc}, TM_{PP}, Bat_{storage}, \Delta SOC) \quad [1\text{-a}]$$

Subject to:

$$50cc \leq ICE_{cc} \leq 130cc \quad [1\text{-b}]$$

$$5\% \leq \Delta SOC \leq 45\% \quad [1\text{-c}]$$

$$HEV\_T_{max,n} \geq ICE_{175cc\text{-}4S}\_T_{max,n} \quad [1\text{-d}]$$

$$SOC_{s\text{-}e} \leq \pm 1\% \quad [1\text{-e}]$$

Only fuel cost savings, battery replacement cost and vehicle capital cost relative to a 175 cc four stroke powered tricycle were considered in the quantification of ICB. Studies have shown that maintenance cost difference between conventional and hybrid electric vehicles is negligible due to maintenance trade-offs between the two systems (Barnitt and Battelle 2006; Ranganathan 2006). Maintenance cost incremental change was thus neglected in the study.

The first constraint indicates the range of engine size considered in the study. Constraint no.3 requires that at all engine speed points ICE and traction motor pairs provide torque peaks comparable to that of a 175 cc four stroke engine ($ICE_{175cc\text{-}4S}\_T_{max,n}$). Constraint no.2 indicates that ΔSOC would have to be within 5% to 45% only.

While $T_{o\text{-}normal}$ and $T_{o\text{-}high}$ are control parameters, they were pegged at 30% and 15% respectively as discussed previously thus were no longer treated as variables. The battery SOC driving start and end difference ($SOC_{s\text{-}e}$) should be limited to avoid charge degradation or accumulation. The fourth constraint limits the average starting and ending state of charge difference to within ± 1%. This is important to avoid battery charge accumulation and degradation.

$$FR = \frac{k(FP)}{HV_{gasoline}} \quad [2]$$

$$FP = \frac{\pi\,(Fmep)(D^2)(L)(n_s)}{4} \quad [3]$$

$$Fmep = \frac{fmep + bmep}{\eta_{th}} \quad [4]$$

Instantaneous Modeling

The parametric engine fuel consumption map utilized in the study was modeled based on basic thermodynamic equations (see Equations 2, 3 and 4).

Fuel power (FP), enrichment factor (k) and fuel heating value ($HV_{gasoline}$) defined instantaneous fuel rate (FR). Fuel power was expressed as a function of the fuel mean effective pressure ($Fmep$), engine speed (n_s), bore (D) and stroke (L). Friction mean effective pressure ($fmep$) was computed based on engine speed, bore, stroke and mean equivalent crankshaft diameter as provided by Yagi et al (1990). The brake mean effective pressure (bmep) was based on the road load requirements and transmission system losses. Thermal efficiency was assumed constant at 30%, typical of common four stroke engines used in tricycles in the Philippines (Biona 2007). The enrichment factor (k) was introduced to account for the effect of fuel enrichment on thermal efficiency during high load modes and was based from Thomas and Ross (1997).

Table 2. EM drive train efficiency (Plotkin et al. 2001)

Component Efficiency	2010	2015	2020
Motor + Inverter	0.92	0.92	0.93
Generator	0.95	0.95	0.96

A gear shift schedule defined by a set of normalized engine rpm and bmep cut-off points calibrated based on actual driver behaviour governed gear shifting decisions (Biona 2007). The engine rpm-bmep curves were modeled based on the 7th order model provided by Nam and Gianelli (2005) for four stroke engines. Transmission losses were simulated using sprocket and gearing power loss analytical models provided by Spicer et al. (2000) and Anderson and Loewenthal (1982) respectively. The transmission system of an RS100 125 cc Yamaha two stroke motorcycle, a unit commonly used in Philippine tricycles, was adopted in the study.

Table 3. Drive cycle characteristics

Parameters	1	2	3	4	5	6
Reference Area	Brgy. Addition Hills [a]	Brgy. San Jose[a]	Sta.Ana[b]	Brgy, Old Zaniga[a]	Brgy. New Zaniga[a]	Kalentong St.[a]
Ave. Speed (kph)	12.76	10.13	21.72	17.84	19.63	15.15
Max. Speed (kph)	19.13	21.50	10.14	31.85	39.80	30.45
Ave. Running Speed (kph)	12.76	10.27	22.10	17.91	20.00	15.18
Maximum Acceleration (m/s^2)	0.90	0.90	1.80	0.70	1.85	1.00
Maximum Deceleration (m/s^2)	1.25	1.20	3.40	1.55	2.25	1.55
Average Acceleration (m/s^2)	0.30	0.36	0.42	0.32	0.40	0.32
Average deceleration (m/s^2)	0.51	0.52	0.58	0.37	0.51	0.36
% Acceleration	44.9%	41.7%	47.6%	29.6%	40.9%	37.5%
% Deceleration	28.3%	29.1%	34.5%	25.1%	32.1%	34.0%
% Cruising	19.7%	24.2%	16.3%	43.4%	26.0%	25.9%
% Idle	6.0%	5.0%	1.6%	1.9%	1.1%	2.6%
Distance (km)	0.66	0.85	4.14	1.32	4.10	1.78

a – Mandaluyong City
b - Manila City

The drive train component efficiencies shown in Table 2 were based on the projected efficiencies for 2010, 2015 and 2020 as provided by Plotkin et al. (2001). Regenerative braking efficiency on the other hand was pegged at 40%.

A Ni-MH battery was adopted. The charging and discharging efficiency behavior of the battery were based from Delucchi et al. (2000). Charging efficiency was expressed as a function of depth of discharge (DOD). Discharge efficiency on the other hand was defined as the product of voltaic and current efficiency. Current efficiency on the other hand was determined based on the open circuit voltage and battery resistance which were both functions of DOD. Battery charging and discharging efficiency and storage capacity deterioration were not quantified in the study.

Performance were evaluated using six (6) driving patterns randomly picked from a database of tricycle speed-time traces in Metro Manila logged using a GPS receiver (Biona 2007). Characteristics of the driving cycles utilized are provided in Table 3.

The first two driving patterns were derived from low income residential areas where roads are narrower and are not as well paved compared to medium income residential areas. Pedestrian activities also often affect vehicle flow in these areas. The next 3 drive cycles on the other hand were gathered from medium income villages. The sixth driving pattern was sourced from a main road where traffic is heavier.

The vehicle road load was computed as the sum of translational inertia, rotational inertia, gradient, rolling friction and air drag loads. The vehicle weight took into consideration the mass of the motorcycle frame, drive train, sidecar, passenger and baggage. Simulations were done assuming 5 passengers weighing 60 kg. with 2 kg baggage allowance each plus the driver. Rolling coefficient of friction was expressed in terms of tire inflation pressure and vehicle speed. A 0.45 air drag coefficient was based on tricycle wind tunnel experiments (Biona 2007). Rotational inertia was quantified by integrating a rotational inertia mass factor to the translational inertia equation (Delucchi et al. 2000).

Component Sizing

As discussed earlier, the traction motor power rating to be paired with an engine is determined based on the torque difference of the engine and the reference tricycle engine (175

Table 4. Drive Train Components Power and Energy Density (Plotkin et al. 2001)

Parameter	2010	2015	2020
Engine Power Density (kg/W)	0.004	0.003	0.003
Motor Power Density (kg/W)	0.003	0.003	0.003
Traction Battery Energy Density (kg/Wh)	0.022	0.021	0.020
Traction Battery Power Density (kg/W)	0.002	0.002	0.002
Transmission Power Density (kg/W)	0.001	0.001	0.001

Table 5. Component cost projections

	2010		2015		2020		
Cost Model (Variable Cost)	Fixed	Variable	Fixed	Variable	Fixed	Variable	Source
Battery ($/kWh)		533		505.5		478	Plotkin et al (2001)
Motor ($/kW peak)	425	21.7	320.5	11.116	216	0.532	Simpson (2006)
Engine ($/kW peak)	41.8	5	41.8	5	41.8	5	Survey of local prices
Transmission ($/kW peak)	54	5	54	5	54	5	Plotkin et al (2001)

Table 6. HEV system configuration for the various engine capacity

Engine Displacement (cc)	50	60	70	80	90	100	110	120	130
ICE Engine peak power (kW)	2.74	3.29	3.84	4.39	4.94	5.48	6.03	6.58	7.13
Motor Peak Power (kW)	9.42	8.66	7.91	7.16	6.40	5.65	4.90	4.14	3.39
Battery Peak Power (kW)	5.82	5.30	4.78	4.32	4.07	3.81	3.56	3.31	3.06
Battery Storage Capacity (kWh)	0.51	0.47	0.42	0.38	0.36	0.34	0.31	0.29	0.27
Component and Vehicle Mass (kg)									
Engine Mass	8.18	9.82	11.46	13.10	14.73	16.37	18.01	19.64	21.28
Traction Motor Mass	28.11	25.86	23.61	21.36	19.11	16.86	14.62	12.37	10.12
Battery Mass	12.07	11.12	10.03	9.05	8.53	8.00	7.47	6.95	6.42
Transmission Mass	9.11	8.95	8.80	8.65	8.49	8.34	8.19	8.03	7.88
Body Mass	98.45	98.45	98.45	98.45	98.45	98.45	98.45	98.45	98.45
Total Vehicle mass	155.92	154.20	152.35	150.61	149.31	148.02	146.73	145.44	144.15

cc four stroke) . Battery capacity on the other hand was selected based on the maximum discharge rate and storage capacity requirements whichever is bigger with the later computed using Equation 5.

$$Bat_{cap} = \frac{P_{d\max}}{\Delta SOC} \qquad [5]$$

The mass of the drive train components were based on the specific weights provided in Table 4.

Drive Train Costing

HEV cost was modeled based on price projections indicated in Table 5. Engine cost was based on a survey of local small engine cost. Considering their high level of technological maturity, no price changes were projected for ICEs. The transmission fixed cost projections provided were modifications of the figures provided by Plotkin et al. (2001) to account for the smaller power requirement in tricycles relative to those originally considered.

Except for the battery life which was modeled as a function of DOD (Milliev et al. 2005) and frequency of charge and discharge cycles, component life was assumed at 250,000 km. Distance traveled per day was set at 100 km with 350 operational days per year (UP-NCTS 2002).

Feasibility Criteria

Considering the limited purchasing capacity of local tricycle operators, the vehicles is expected to be mostly through micro-financing. On the average, micro-financing institutions levy monthly interest rates between 2% to 3%. HEVs will only be attractive to the sector if it will be able to provide a net increase in daily income over and above the monthly amortization. The minimum attractive rate of return for HEVs was thus set at 5% per month. Future local fuel cost was assumed to be linearly related with world crude oil prices as indicated in ADB (2008).

RESULTS AND DISCUSSION

HEV Component Sizing Configuration

Implementation of the component sizing process yielded the system configurations shown in Table 6. The component weights indicated were based on the 2015 energy density data.

The succeeding section details the optimum settings and performance that each of these system configurations could provide.

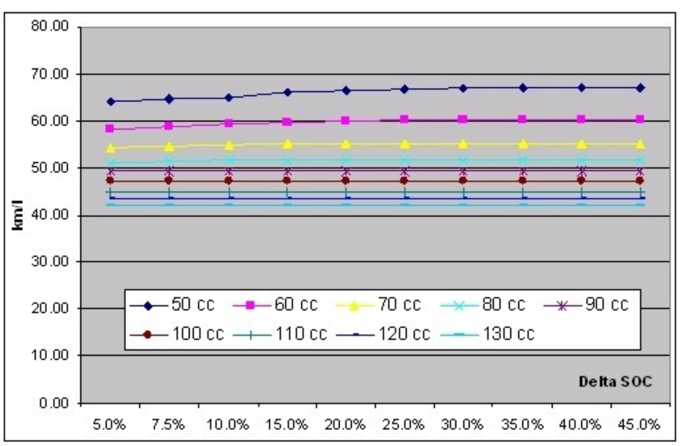

Figure 2. ∆SOC – Fuel Economy relationship for various engine power configuration in 2015

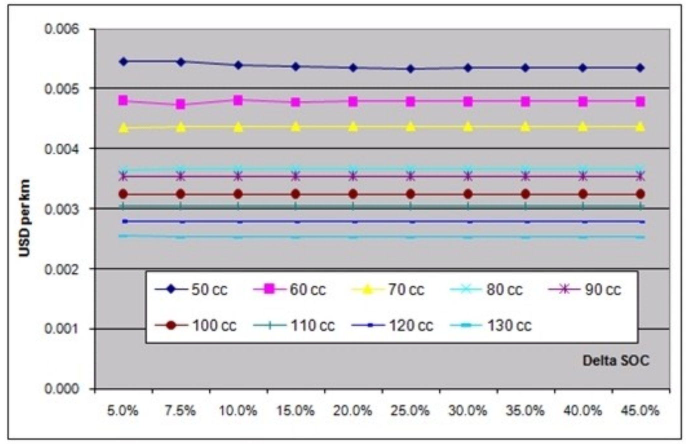

Figure 3. ∆SOC -Battery cost per km. relationship for various engine power configuration in 2015

Optimum ∆SOC Setting

Increasing *∆SOC* generally led to slight increases in fuel economy (See Figure 2).This could be attributed to two factors. First, increasing *∆SOC* leads to lower SOC before ICE based charging is triggered (SOC_{min}) limiting the fuel utilized to charge the battery. Second, a lower SOC_{min} also increases the duration by which the electric motor power the vehicle at low torque points thus maximizing the benefits of the electric power train.

While battery capacity does not vary with *∆SOC* for a given drive train configuration, *∆SOC* affects the battery charging cycle and depth of discharge (DOD) which translates to effects in battery replacement frequency. Note that ICE based charging is triggered when SOC_{min} is reached. Setting a limited *∆SOC* brings up SOC_{min} which leads to more frequent charging cycles (see Figure 3). This effect however is more pronounced in predominantly EM (50 cc and 70 cc) and predominantly ICE (120 and 130 cc) engine configurations. For predominantly EM configurations, charging and discharging frequency are more

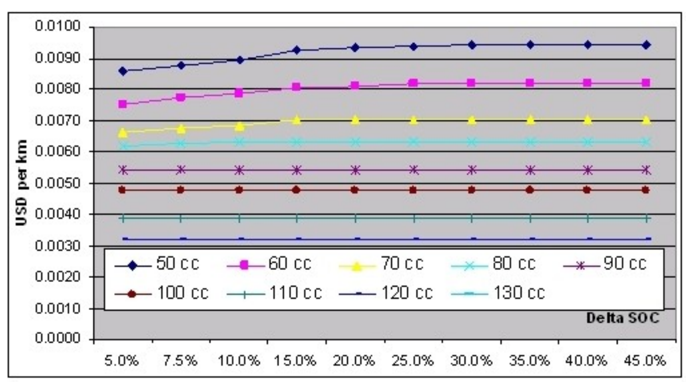

Figure 4. ∆SOC – incremental HEV cost benefit per km. relationship for various engine power configuration in 2015

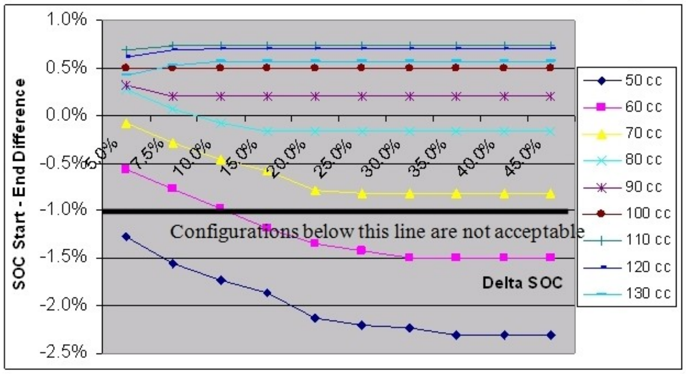

Figure 5. ΔSOC – SOC start / end difference in 2015 for various engine configuration

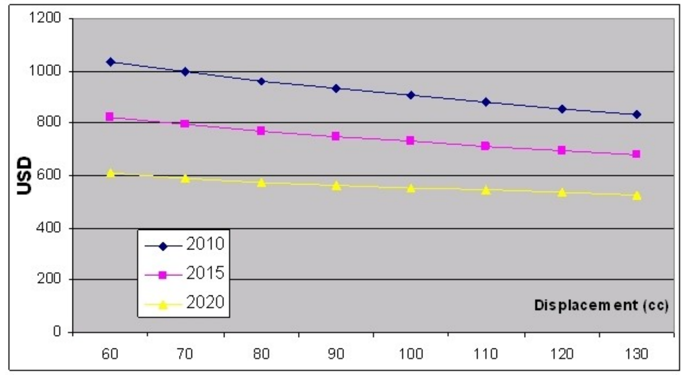

Figure 6. Drive train capital cost for various system configuration

Table 7. Optimum ΔSOC

Engine Displacement (cc)	60	70	80	90	100	110	120	130
Optimum ΔSOC	10%	≥30%	≥30%	≥30%	≥30%	≥30%	≥30%	≥30%

Table 8. Fuel economy for various system configuration in km./l

	Engine Capacity (cc)							
Year	60	70	80	90	100	110	120	130
2010	58.35	55.08	51.30	48.85	46.72	44.56	42.84	41.28
2015	58.62	55.33	51.57	49.21	47.11	44.93	43.27	41.77
2020	58.72	55.38	51.62	49.30	47.15	44.98	43.31	41.81

sensitive to control settings as the electric drive train provides a big part of its power requirement. Predominantly ICE configurations on the other hand are equipped with smaller capacity batteries providing a limited operational range between SOC_{max} and SOC_{min}. This makes charging and discharging cycle frequencies more sensitive to ΔSOC.

Results indicated that the positive effects of utilizing higher ΔSOC on fuel economy offset its higher battery cost implications. This is shown in Figure 4 where the incremental cost benefits of hybridization increase with ΔSOC.

In all configurations, the HEV cost benefit per kilometer increases until the ΔSOC = 30% point where no further improvement is observed thereafter. Since increasing ΔSOC increases the operational share of the EM component, high ΔSOC could lead to battery storage depletion which is undesirable. To satisfy constraint no.4, ΔSOC for the 60 cc configuration could not go higher than 10% while no ΔSOC limit was found for higher engine capacity systems. The 50 cc system configuration may not be used as it failed to satisfy the limit (see Figure 5). This is true unless battery capacity is

Table 9. Fuel economy improvement comparison with other studies

Reference	F.E. Improvement
This Study	
Maximum	76%
Minimum	24%
Other Studies:	
Baumann et al. (2000)	16.0%
Lin et al (2001)	28.2%
Butler et al. (1999)	145.4%
Butler et al. (1999)	33.1%
Arsie et al (2004)	69.4%
Lin et al (2003)	45.0%
Average (other studies)	**56.2%**

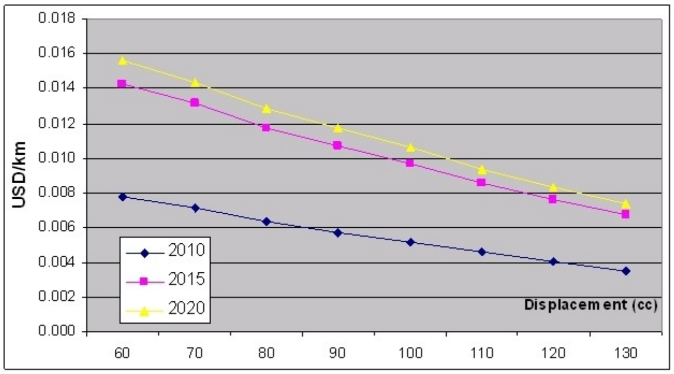

Figure 7. Incremental fuel cost benefits for various system configuration

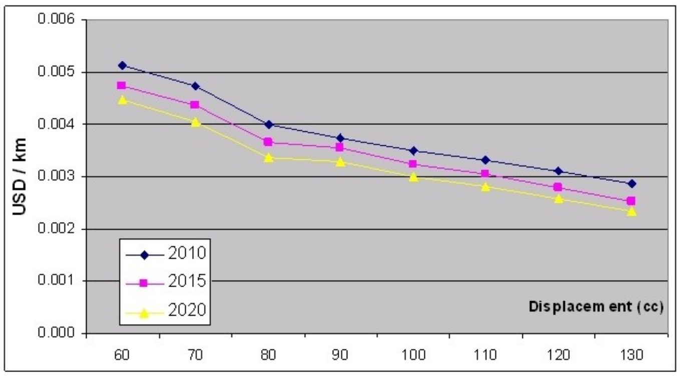

Figure 8. Incremental battery cost per km for various system configuration

increased beyond what is just needed to satisfy charge and power requirements. Increasing the battery sizes of the 50 cc and 60 cc systems however is not financially practical.

Based on the cost benefits and constraints considered, the optimum ΔSOC settings for the various system configurations are summed up in Table 7. The 50 cc configuration was not included for reasons discussed earlier.

Incremental Cost and Viability

The 2010, 2015 and 2020 drive train capital costs are provided in Figure 6. As expected, capital cost is highest in 2010 and lowest in 2020 as the HEV market become more mature and main stream. Drive train cost reductions between 2010 to 2020 have been projected to be between 70% (for 60 cc system) to 60% (for 130 cc system). Capital requirements increases as the EM component of the system is increased as in the case of lower capacity engine configurations. This effect however is weaker in 2020 when HEV component cost are expected to be lower.

Fuel economy varies significantly across the system configuration evaluated. It ranged from as high as 58.72 km/l for the 60 cc configuration to as low as 41.81 km/l for the 130 cc engine system (see Table 8).

These figures correspond to 76% to 24% improvements relative to the 33.28 km/l fuel economy of the baseline system (175 cc four stroke conventional units). These results are well within the range of improvements recorded in other studies (see Table 9).

ICE operation duration share for EM dominated configurations (smaller engine capacity systems) are limited thus their better fuel economy. While improvements in fuel

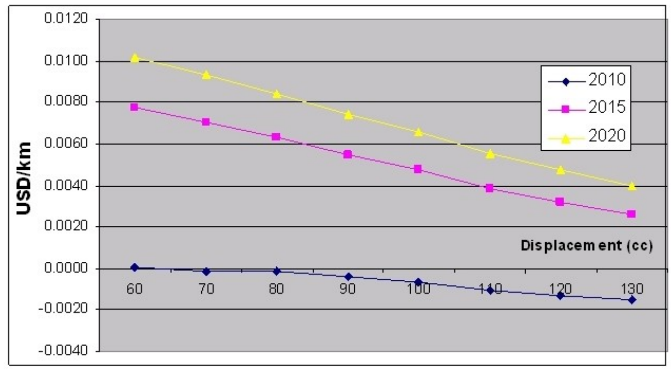

Figure 9. Incremental life cycle cost benefits for various engine displacement

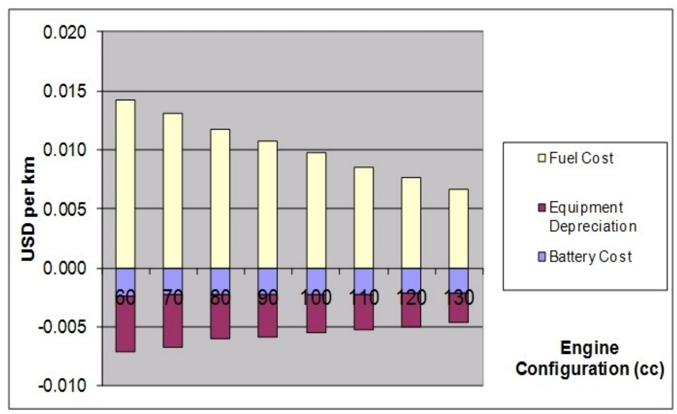

Figure 10. Incremental life cycle cost benefits breakdown for various system configuration in 2015

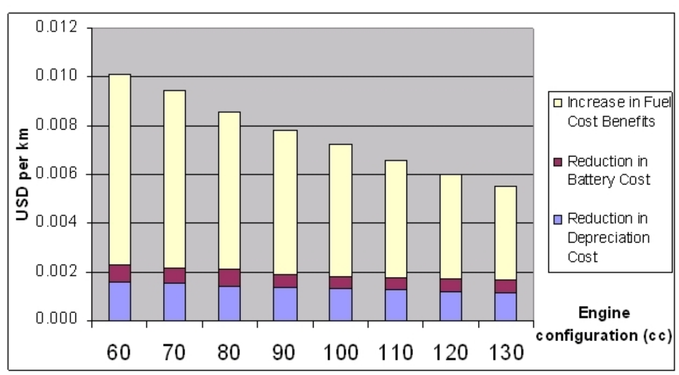

Figure 11. Incremental life cycle cost benefits improvement breakdown (2010-2020)

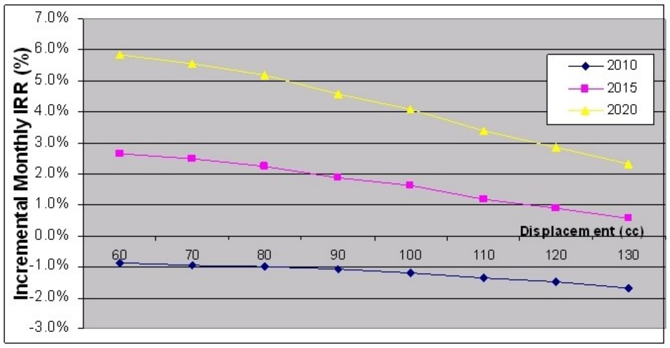

Figure 12. Monthly internal rate of return for various engine displacement

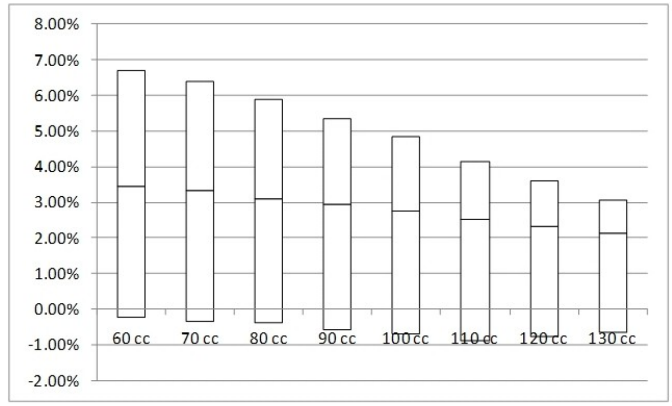

Figure 14. Monthly rate of return – fuel price sensitivity for 2015

increases (ADB 2008) are expected to double fuel cost benefit between 2010 to 2020 (see Figure 7).

Incremental battery costs are lower for predominantly ICE systems (see Figure 8) where battery capacities are smaller (see Table 1). Incremental battery cost reductions from 2010 to 2020 effected by decreasing specific cost and improvements in energy and power density will be between 15% to 22% (see Figure 8). This is expected to contribute significantly in the viability of hybrid tricycles in the future.

The over-all incremental benefit of the HEV technology in tricycles was found to be higher in EM dominated systems as shown in Figure 9. A breakdown of the incremental cost is provided in Figure 10. The increased viability of the technology in the future could be attributed mostly to increase in fuel cost benefits (see Figure 11). The future viability of HEV technology in tricycles is thus hinged on oil prices more than anything else.

The 60 cc system is expected to provide the most incremental cost benefits among all configurations evaluated. Simulation results also indicate that the HEV technology will not be financially practical for tricycles in 2010.

It will be financially viable for tricycles only by 2020 based on a monthly minimum attractive interest rate (MARR) of 5% (see Figure 12). This viability will be limited only to EM dominated systems (60 cc, 70 cc and 80 cc). Considering the environmental benefits that the technology provide, the provision of soft loans to facilitate its adoption in tricycle to as early as 2015 should be considered.

As discussed earlier, fuel price will dictate the viability of the technology. The sensitivity of the monthly internal rate of return (IRR) with fuel prices were simulated and provided in Figures 13, 14 and 15. Fuel price were set at $ 0.60, $ 1.20 and $ 1.80 per liter representing the upper, mode and lower monthly IRR values indicated in the graphs. It could be noted that not even the upper fuel cost limit is enough to provide viability to any of the configurations in 2010 (see Figure 13).

A fuel cost of $ 1.80 per liter will make the 60 cc to 90 cc viable by 2015. This viability range is further expanded in 2020 to include all configurations. It could be noted also that the projected system cost reductions and performance improvement in 2020 will be enough to provide financial viability for the 60 cc to 80 cc systems even only at $ 1.20 per liter fuel cost. Results also indicated that the monthly IRR of electric motor

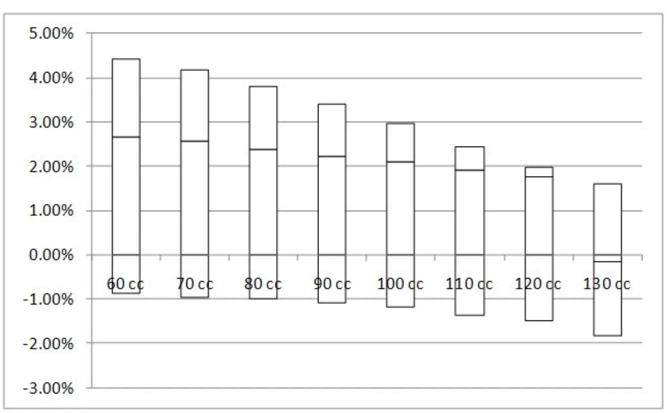

Figure 13. Monthly rate of return – fuel price sensitivity for 2010

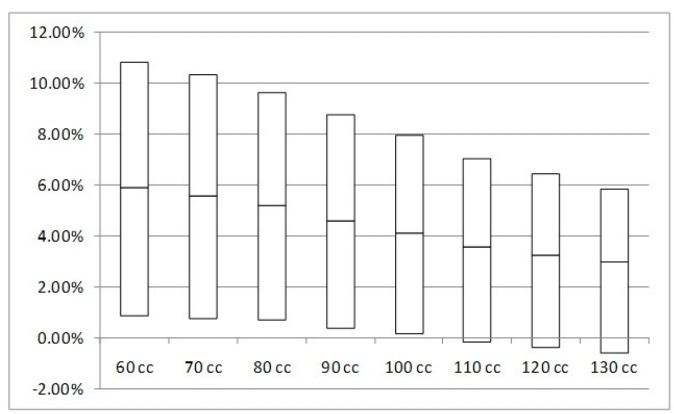

Figure 15. Monthly rate of return – fuel price sensitivity for 2020

dominated systems (lower engine sizes) are more sensitive to fuel cost (see Figure 14).

CONCLUSIONS

An instantaneous model for the determination of the performance and cost benefits of the HEV technology in Philippines tricycles was developed. Appropriate HEV component sizes for 50 cc to 130 cc engine configurations were determined and evaluated. Results of the simulations are summarized as follows:

- ΔSOC affects fuel economy and battery cost which translates to influences on over-all cost benefits of the HEV technology in tricycles. Increasing ΔSOC generally slightly increases fuel economy and decreases battery cost. The HEV cost benefits peaks at the ΔSOC=30% with no further improvement expected beyond it. Higher ΔSOC on the other hand widens the starting and ending SOC difference which is technically undesirable. This effect is more significant in EM dominated systems and limits feasible ΔSOCs for the 60 cc configuration to a maximum of 10%. It also renders the 50 cc configuration technically unacceptable.
- Capital and battery replacement cost increases with increasing EM share (decreasing engine capacity configuration). An opposite relationship is expected between fuel cost benefits and increasing EM share. The adoption of the HEV technology in tricycles could increase fuel economy to between 41.5 to 58.5 km/l from 33.28 km/l (175 cc 4 stroke units). The 60 cc ICE HEV configuration provides the best fuel economy and highest financial feasibility while the 70 cc and 80 cc systems may also be adopted should lower capital cost is desired.
- The adoption of the HEV technology in tricycles becomes feasible only in 2020. The net economic benefits of the technology by 2015 will not be enough to financially justify its adoption unless soft loans are provided. The technology is not expected to provide positive economic benefits in 2010.
- The projected fuel price increases in the future is expected to dictate the viability of the HEV technology in tricycles more than projected performance improvements and component cost reductions.

The points cited were obtained based on the assumption that fuel prices will increase linearly and finally double by 2020 from the $ 0.60 per liter price of 2010. Viability was evaluated relative to a 175 cc four stroke engine powered tricycles. It is recommended that evaluation is done also relative to other future drive trains such as 100% electric systems.

NOMENCLATURE

ICB	Incremental Life Cycle Cost Benefits
ICE_{cc}	ICE Displacement Volume
TM_{PP}	Traction Motor Peak Power
$Bat_{storage}$	Battery Storage Capacity
ΔSOC	State of Charge Operational Range
$HEV\_T_{\max,n}$	HEV Maximum Torque at n rpm
$ICE_{175cc-4S}\_T_{\max,n}$	175 cc four stroke maximum Torque at n rpm
FR	Instantaneous Fuel Rate
k	Enrichment Factor
FP	Fuel Power
Bat_{cap}	Battery Storage Capacity
$P_{d\max}$	Maximum Power Discharge

ACKNOWLEDGEMENT

The Authors wish to thank the University Research and Coordination Office (URCO) of De La Salle University – Manila for the grant provided that made possible the conduct of the study.

NO CONFLICT OF INTEREST STATEMENT

We certify that there is no conflict of interest or financial conflict in the conduct of the present study, in the preparation or submission of this manuscript.

CONTRIBUTIONS OF INDIVIDUAL AUTHORS

Jose Bienvenido Manuel M. Biona

Main researcher and author of the study. The design optimization process was implemented using the " Tricycle Energy Emissions Model" or TEEM he developed in his Doctoral Dissertation research at De La Salle University-Manila.

Alvin B. Culaba

He contributed in the conceptualization of TEEM and the design optimization process. He also evaluated the results of the optimization work for validity and accuracy. He is the adviser of the main author in his doctoral dissertation work.

REFERENCES

ADB. Part 2 - Global Commodity Price Rises and Impacts on Developing Asia. In: Asian Development Outlook 2008 Update. Mandaluyong City: Asian Development Bank, 2008: 30-72.

Anderson NE, Loewenthal SH. Design of spur gear for improved efficiency. ASME J Mech Des 1982; 104: 767–774.

Arsie I, Graziosi M, Pianese C, Rizzo G, Sorrentino M. Optimization of Supervisory Control Strategy for Parallel

Hybrid Vehicle with Provisional Load Estimate. In: AVEC 2004; 483-488.
Assanis D, Delagrammatikas G, Fellini R, Filipi Z, Liedtke J, Michelena N, Papalambros P, Reyes D, Rosenbaum D, Sales A, Sasena M. An Optimization Approach to Hybrid Electric Propulsion System Design. Mech Struc Mach 1999; 27(4): 393-421.
Barsali S, Miulli C, Possenti A. A Control Strategy to Minimize Fuel Consumption of Series Hybrid Electric Vehicles. IEEE Trans Energy Convers 2004; 19 (1):187-195.
Barnitt R, Battelle KC. New York City Transit (NYCT) hybrid (125 order) and CNG transit buses final evaluation results. Boulder, Colorado: National Renewable Energy Laboratory, 2006, (NREL/TP-540-40125).
Butler K, Ehsani M, Kamath P.A Matlab-based modeling and simulation package for electric and hybrid electric vehicle design. IEEE Trans Veh Des 1999; 48 (6):1770-1778.
Baumann B, Washington G, Glenn B, Rizzoni G. Mechatronic Design and Control of Hybrid Electric Vehicles. IEEE/ASME Trans Mechatron 2000; 5(1): 58-72.
Biona, J B M. Possibilistic dynamic life cycle assessment based energy and emissions model for Philippine tricycles. Ph.D. Dissertation. De La Salle University-Manila, 2007.
Delucchi M., Burke A, Lipman A, Miller M. Electric and gasoline vehicle lifecycle cost and energy-sue model. Davis, California: Institute of Transportation Studies – University of California Davis, 2006, (Final Report No. UCD-ITS.RR-04).
Garcia D, Ong A, Villanueva M, Cleto M, Sioson K, Lidasan H. Assessment of tricycle system as an access mode for to-work trips in metropolitan areas: The case of Quezon City. Paper delivered at the 15th Annual Conference of the Transportation Science Society of the Philippines. Mandaluyong City, December 7, 2007. Available at http://www.eesi.org/files/eesi_hybrid_bus_032007.pdf. Accessed 2009 June 3.
Johnson V, Wipke K, Rausen D. HEV Control Strategy for Real Time Optimization of Fuel Economy and Emissions. Warrendale, Pennsylvania: Society of Automotive Engineers, 2000, (SAE 2000-01-1543).
Lin CC, Kang JM, Grizzle J, Peng H. Energy Management Strategy for a Parallel Hybrid Electric Truck. In: Proceedings of the American Control Conference, Arlington, Virginia, June 25-27, 2001; 4: 2878-2883.
Lin CC, Peng H, Grizzle J, Liu J, Busdiecker M. Control System Development for an Advanced-Technology Medium-Duty Hybrid Electric Truck. Warrendale, Pennsylvania: Society of Automotive Engineers, 2003, (SAE No. 03TB-45).
Milliev JM, Mcleer P, Everett M, Strangas E. Ultracapacitor plus battery energy storage system sizing methodology. Paper delivered at the IEEE ISIE Conference. Dubrovnik, June 20-23, 2005.
Montazeri-Gh M, Poursamad A. Application of Genetic Algorithm for Simultaneous Optimization of HEV Component Sizing and Control Strategy. Int J Altern Propul 2006; 1 (1): 63-78.
Nam E, Gianelli R. Fuel consumption modeling of conventional and advanced technology vehicles in the physical emission rate estimator. Washington, DC: United States Environmental Protection Agency, 2005, (EPA420-P-05-001).
Plotkin S, Santini D, Vyas A, Anderson J, Wang M, He J, Bharathan D. Hybrid Electric Vehicle Technology Assessment: Methodology, Analytical Issues, and Interim Results. Argonne, Illinois: Argonne National Laboratory, 2001, (ANL/ESD/02-2).
Ranganathan S. Hybrid Buses Costs and Benefits. Washington D.C.: Environmental and Energy Study Institute, 2006. Available at http://www.eesi.org/files/eesi_hybrid_bus_032007.pdf. Accessed 2009 May 20.
Rebitzer G, Loerincik Y, Jolliet O. Input–output life cycle assessment: from theory to applications. Int J LCA 2002; 7:174–6.
Senthil KD, Ong SK, Nee AYC, Tan BH. A proposed tool to integrate environmental and economical assessments of products. Environ Impact Assess Review 2003; 23:51–72.
Shouten NJ, Salman MA, Kheir NA. Fuzzy control for parallel hybrid vehicles. IEEE Trans Control Syst Technol 2002; 10(3): 460-468.
Simpson A. Cost Benefit Analysis of Plug-in Hybrid Electric Vehicle Technology. Paper delivered at the 22nd International Battery, Hybrid and Fuel Cell Electric Vehicle Symposium and Exhibition. Yokohama, Oct.23-28, 2006.
Spicer BC, Richardson JKC, Ehrlich JM, Bernstein JR. On the efficiency of bicycle chain drives. Tech J IHPVA 2000; 50, 3–9.
Thomas M, Ross M. Development of second-by-second fuel use and emissions models based on an early 1990s composite car. Warrendale, Pennsylvania: Society of Automotive Engineers, 1997, (SAE 971010).
UP-NCTS . Standards Development for Local Motorcycle/Tricycles-3rd Quarter Progress Report. Diliman, Quezon City: National Center for Transportation Studies-University of the Philippines, 2002.
Wang, M. Development and Applications of GREET 2.7 – The Transportation Vehicle-Cycle Model. Center for Transportation Research. Energy Systems Division. Argonne, Illinois: Argonne National Laboratory, 2007. Available at http://www.transportation.anl.gov/modeling_simulation/GREET/publications.html. Accessed 2007 August 15.
Yagi S, Ishibasi Y, Sono H. Experimental analysis of total engine friction in four stroke S.I. engines. Warrendale, Pennsylvania: Society of Automotive Engineers, 1990, (SAE 900223).